Short-delayed-feedback semiconductor lasers

Anton V. Kovalev* and Evgeny A. Viktorov
ITMO University, Birzhevaya Liniya 14, 199034 Saint Petersburg, Russia

Thomas Erneux
Université Libre de Bruxelles, Optique Nonlinéaire Théorique, Campus Plaine C.P. 231, 1050 Bruxelles, Belgium

(Received 26 September 2020; accepted 22 March 2021; published 12 April 2021)

We consider the laser rate equations describing the evolution of a semiconductor laser subject to an optoelectronic feedback. We concentrate on the first Hopf bifurcation induced by a short delay and develop an asymptotic theory where the delayed variable is Taylor expanded. We determine a nearly vertical branch of strongly nonlinear oscillations and derive ordinary differential equations that capture the bifurcation properties of the original delay differential equations. An unexpected result is the need for Taylor expanding the delayed variable up to third order rather than first order. We discuss recent laser experiments where sustained oscillations have been clearly observed with a short-delayed feedback.

DOI: 10.1103/PhysRevE.103.042206

I. INTRODUCTION

Many lasers and especially semiconductor lasers are extremely sensitive to delayed optical feedbacks. First considered as nuisances, such feedbacks have led to practical applications ranging from encrypted communications to new sensing devices. During the 1980s, and even more in the 1990s, combined experimental and theoretical studies of laser instabilities caused by the delay have boosted research activities of nonlinear delay dynamical systems in general [1–5]. In nonlinear optics, Ikeda was the first to show that the delay not only controls the instability threshold but also the detailed shape of the resulting oscillations [6,7]. While this effect can be rather striking in the often-studied case of long delays in the feedback loop [8,9], Ikeda *et al.* have also shown that optical chaos does persist, even when the delay time is comparable to or even smaller than the system's response time. While it is relatively easy to understand the mechanism by which the instability disappears as the delay becomes sufficiently small, it is much harder to anticipate possible dynamical instabilities when competing physical phenomena evolve over comparable timescales [10,11].

Two specific feedback problems have revived the interest of the short delay limit of delayed-feedback lasers. For a semiconductor laser (SL) subject to an optical feedback (OF) from a distant mirror, it has been shown that, if the feedback round-trip time is sufficiently short, regular pulses are observed instead of chaotic signals [12–15]. Recently, reservoir computing has been experimentally demonstrated using an integrated circuit with a semiconductor laser and a short optical feedback [16]. Short external round-trip times are naturally present in integrated photonic circuits [17,18]. More recently, SLs subject to an optoelectronic feedback (OEF) have been studied as promising sources of spectrally pure microwave signals [19,20]. The laser is driven by an injection current, which can be modulated by a delayed OEF. By contrast to optical feedback, the effects of both positive and negative feedback can be investigated since the current proportional to the detected optical power can be added or subtracted from the laser pump current. A negative OEF is particularly interesting because it generates regular pulses for moderate feedback gains and delays [4,21].

Compared to the OF case, the laser equations for the OEF problem are much simpler and have stimulated analytical studies [22–24]. These equations have been explored in the limit of small feedbacks but arbitrary delays and revealed the emergence of both bifurcating and isolated branches of periodic solutions [22–24]. The objective of this paper is to analyze the limit of small delays but arbitrary feedback amplitudes. This limit can be realized experimentally by controlling the relaxation oscillation (RO) frequency relative to the delay frequency as has been realized in Ref. [18]. The ROs are slowly decaying intensity oscillations of the laser in the absence of any external fixed perturbations. This slow damping can be explained mathematically but requires a major reformulation of the laser equations as the equations of a weakly damped conservative oscillator. As we shall demonstrate, a Hopf bifurcation to strongly nonlinear oscillations is possible if the delay is comparable in magnitude to the damping rate of the ROs. The asymptotic analysis is not a routine application of singular perturbation methods because its success depends on a Taylor expansion of the delayed variable up to third order.

In dimensionless form, a SL with a negative OEF is described by the following two equations for the intensity of the laser field I and the carrier density N [24,25]:

$$I' = 2NI, \tag{1}$$

$$TN' = P + \eta I(t-\tau) - N - (1+2N)I. \tag{2}$$

*avkovalev@niuitmo.ru

Time t and delay τ are measured in units of the photon lifetime ($t \equiv t'/\tau_{ph}$ and $\tau \equiv \tau_d/\tau_{ph}$). $P \sim J - J_{\rm th}$ is the dimensionless pump parameter above threshold in the absence of feedback ($\eta = 0$). J and $J_{\rm th}$ denote the injection current and its threshold value for lasing. $T \equiv \tau_c/\tau_{ph}$ is the ratio of the carrier and photon lifetimes. $\eta < 0$ and τ represent the dimensionless gain and delay of the OEF, respectively. Typical values for τ_{ph} and τ_c are 10^{-11} s and 10^{-9} s, respectively, which implies $T = 10^2$. This means that N evolves on a much slower timescale than I. Experimentally recorded delays τ_d are in the 10^{-9} s range, which gives $\tau = 10^2$.

The plan of the paper is as follows: In Sec. II, we formulate the laser rate equations and proceed to a bifurcation analysis where the delayed variable is Taylor expanded to first order. We find that the Hopf bifurcation is vertical in first approximation. It motivates a higher-order analysis detailed in Sec. III where we need to expand the delayed variable up to third order. We obtain the bifurcation equation, which relates amplitude and period of periodic solutions to control parameters. Our analysis suggests a minimal set of ordinary differential equations (ODEs), which we formulate in Sec. IV. We compare the numerical bifurcation diagrams of the delay differential equation (DDE) and ODE systems and find quantitative agreement. Finally, we summarize previous mathematical attempts on the short delay limit and discuss recent laser experiments using a short delay feedback.

II. DELAYED-FEEDBACK LASER EQUATIONS

In this section, we plan to reformulate Eqs. (1) and (2) as a weakly perturbed conservative system of equations. To this end, precious information is obtained by analyzing the limit of small delays of the Hopf bifurcation conditions. The nonzero intensity steady state of Eqs. (1) and (2) is given by

$$(I, N) = \left(\frac{P}{1-\eta}, 0\right), \tag{3}$$

and its linear stability is found by solving the following characteristic equation for the growth rate λ:

$$\lambda^2 T + \lambda(1 + 2I) - 2I[\eta \exp(-\lambda\tau) - 1] = 0. \tag{4}$$

The stability boundaries delimiting the domains of stability in parameter space are Hopf bifurcation points. Inserting $\lambda = i\sigma$ into Eq. (4) and separating the real and imaginary parts lead to the following equations:

$$\sigma^2 T + \frac{2P}{1-\eta}[\eta\cos(\sigma\tau) - 1] = 0, \tag{5}$$

$$\sigma(1 - \eta + 2P) + 2P\eta\sin(\sigma\tau) = 0. \tag{6}$$

We wish to solve these equations in terms of P and τ. To this end, we introduce $z \equiv \sigma\tau$ and reformulate Eqs. (5) and (6) in terms of z. We obtain

$$\frac{z^2}{\tau^2} T + \frac{2P}{1-\eta}[\eta\cos(z) - 1] = 0, \tag{7}$$

$$\frac{z}{\tau}(1 - \eta + 2P) + 2P\eta\sin(z) = 0. \tag{8}$$

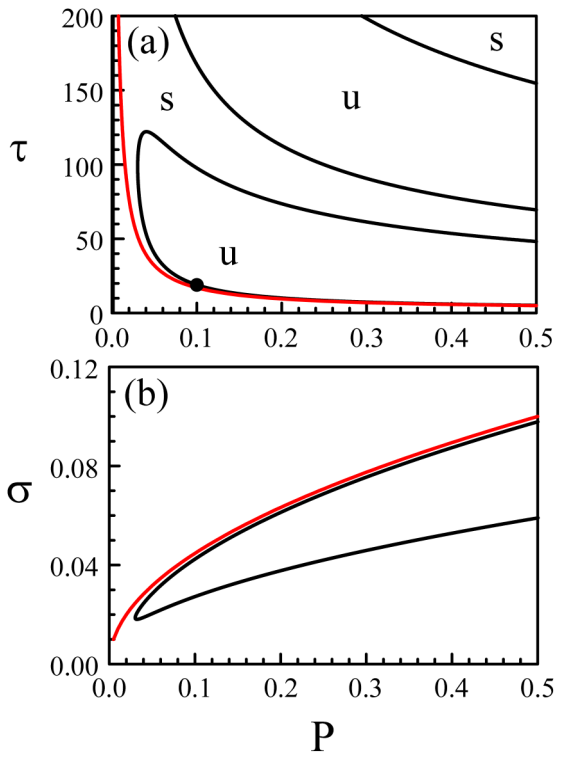

FIG. 1. (a) Hopf bifurcation lines delimiting the domains of stability. They are obtained from the parametric solution (9) and (10) by gradually increasing z from 0 to 3π. The red line is the approximation (12). The fixed parameters are $T = 100$ and $\eta = -0.5$. The dot marks the Hopf bifurcation point at $(P, \tau) = (0.1, 18.98)$. s and u mean stable and unstable steady state, respectively. (b) Hopf frequencies. There are only two branches of frequencies. The red line is the RO frequency (14).

We are now ready to derive a parametric solution for $\tau = \tau(P)$ (parameter z). From Eq. (8), we determine $P > 0$ as

$$P = -\frac{1}{2}\frac{z(1-\eta)}{z + \eta\tau\sin(z)}. \tag{9}$$

Substituting Eq. (9) into Eq. (7), we obtain a quadratic equation for τ given by

$$\tau^2[1 - \eta\cos(z)] + \tau\eta\sin(z)Tz + z^2T = 0. \tag{10}$$

We next proceed as follows: We continuously increase $z > 0$ from zero, determine $\tau > 0$ from Eq. (10), and then P from (9). See Fig. 1(a). An approximation of the Hopf bifurcation line for low values of τ can be obtained in the large-T limit by assuming $z = O(T^{-1/2})$ but keeping τ and P as $O(1)$ quantities. From Eq. (9), we find

$$P = -\frac{1-\eta}{2(1+\eta\tau)} \quad (\eta < -\tau^{-1}), \tag{11}$$

or equivalently,

$$\tau = -\frac{1}{\eta}\left(\frac{1-\eta}{2P} + 1\right). \tag{12}$$

Moreover, from Eq. (10) with $z = O(T^{-1/2})$, we obtain the leading approximation of z^2

$$z^2 = \frac{-\tau^2(1-\eta)}{T(1+\eta\tau)}. \tag{13}$$

Using Eq. (11) and then $z^2 = \sigma^2\tau^2$, we determine σ as

$$\sigma = \sqrt{\frac{2P}{T}}. \tag{14}$$

The frequency (14) is the relaxation oscillations (RO) frequency of the free-running laser [25]. Figure 1(b) represents the Hopf bifurcation frequencies. There are only two branches for all bifurcations lines and we explain why in the Appendix.

We now concentrate on the first Hopf bifurcation as we increase τ from zero. It admits the approximation (12), and its frequency is close to the RO frequency (14).

A. Reformulation

We learned from the previous section that the RO frequency (14) is the frequency of the first Hopf bifurcation. It is therefore important to reformulate the laser equations (1) and (2) in terms of the RO timescale. To this end, we introduce x and y as the deviations of I and N from their steady state values (3), and a new time s. They are defined by

$$I = \frac{P}{1-\eta}(1+y), \quad N = \frac{\omega}{2}x \text{ and } s = \omega t, \tag{15}$$

where

$$\omega \equiv \sqrt{\frac{2P}{T(1-\eta)}} \tag{16}$$

is a rescaled RO frequency. The new time s and the coefficients of x and y are determined by requiring that the large T parameter multiplying N' in Eq. (2) is eliminated and by having no parameters left in the equation for y. The factor $1-\eta$ in Eq. (16) allows us to further simplify the equation for x. Inserting Eq. (15) into Eqs. (1) and (2), we obtain

$$y' = x(1+y), \tag{17}$$

$$x' = -y + \eta y(s-\theta) - \varepsilon x\left(1 + \frac{2P}{1-\eta}(1+y)\right), \tag{18}$$

where

$$\varepsilon \equiv \sqrt{\frac{1-\eta}{2PT}} \ll 1 \text{ and } \theta \equiv \omega\tau. \tag{19}$$

Equations (17) and (18) offer several advantages compared with the original laser rate equations (1) and (2). First, the large parameter T is no longer multiplying a time derivative of a dependent variable but now appears as a small perturbation term through ε. Second, setting $\varepsilon = 0$ provides a reduced problem where only the feedback parameters appear. As we shall detail, these equations exhibit conservative oscillations in the limit of small delays.

Mathematically, the delay θ is the most convenient bifurcation parameter since it only appears in the delayed variable. Experimentally, it is the pump parameter P, which is the control parameter. According to Eq. (16) and the definition of θ in Eq. (19), decreasing P decreases θ. Changing P, however, modifies both θ and ε, as well as the last term in Eq. (18). We are going to use θ in our bifurcation analysis of Eqs. (17) and (18) and consider either θ or P as control parameters in all our numerical simulations. Figure 2 shows the long-time evolutions of y when the bifurcation parameter is increased above its Hopf bifurcation value. The transition from nearly harmonic to pulsating oscillations occur quite rapidly as we slightly change the control parameter. More precisely, strong pulses appear as soon as the minimum of y approaches $y = -1$ (corresponding to $I = 0$). Both the maxima of y and the interpulse period increase as we increase the control parameter from its bifurcation point. The bifurcation diagrams of the extrema of y are shown in Fig. 3.

Equations (17) and (18) are equivalent to those derived in Refs. [22,23] except that the feedback rate η is now considered as an $O(1)$ quantity rather than being $O(\varepsilon)$ small. The nonzero intensity steady state of Eqs. (17) and (18) is $(x, y) = (0, 0)$ and, from the conditions for a Hopf bifurcation, we find that the first Hopf bifurcation exhibits a frequency

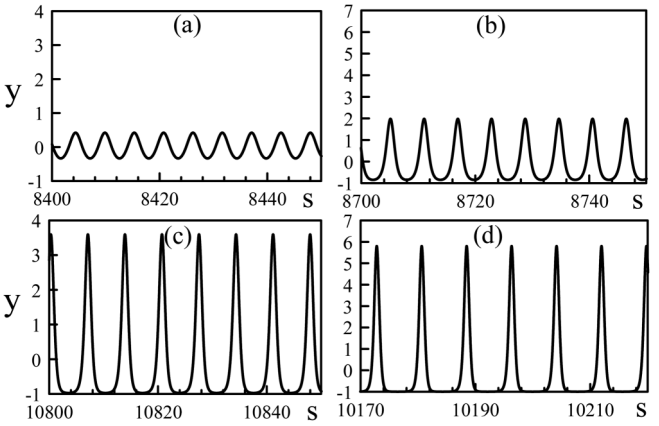

FIG. 2. From harmonic to pulsating oscillations. Long-time numerical solutions of Eqs. (17) and (18). (a), (c) $T = 100$, $\eta = -0.5$, $P = 0.1$, implying $\omega = 0.04$ and $\varepsilon = 0.27$. (a) $\theta = 0.7$ ($\tau = 19.17$) and (b) $\theta = 0.9$ ($\tau = 26.65$). The Hopf bifurcation point is at $\theta = 0.693$ ($\tau = 18.98$) and corresponds to the dot in Fig. 1. (b), (d) $T = 100$, $\eta = -0.5$, and $\tau = 18.90$. (b) $P = 0.11$ and (d) $P = 0.15$. The Hopf bifurcation point is located at $P = 0.1004$.

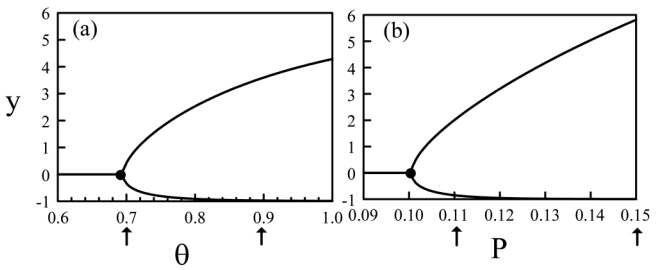

FIG. 3. Bifurcation diagram of the extrema of y. (a) $T = 100$, $\eta = -0.5$, and $P = 0.1$. The Hopf bifurcation point is at $(\theta, y) = (0.693, 0)$. (b) $T = 100$, $\eta = -0.5$, and $\tau = 18.90$. The Hopf bifurcation point is at $(P, y) = (0.1004, 0)$. The arrows indicate the values of either θ or P corresponding to the time traces shown in Fig. 2.

$\sigma = 1 - \eta + O(\varepsilon^2)$ and is located at

$$\theta = \varepsilon\theta_1 + O(\varepsilon^3), \tag{20}$$

where

$$\theta_1 = -\frac{1-\eta+2P}{\eta(1-\eta)} \ (\eta < 0). \tag{21}$$

In terms of $\tau = \theta/\omega$, Eq. (20) is identical to Eq. (12).

B. Small-delay limit

The approximation of the Hopf bifurcation point (20) is an $O(\varepsilon)$ small quantity. It suggests to expand the delayed variable $y(s-\theta)$ in Eq. (18) for small θ. We find

$$x' = -y + \eta[y - \theta y' + O(\theta^2)] - \varepsilon x\left[1 + \frac{2P}{1-\eta}(1+y)\right]. \tag{22}$$

Assuming $\theta = O(\varepsilon)$ and seeking a solution in power series of ε leads to the following reduced problem for x and y:

$$y_0' = x_0(1+y_0), \tag{23}$$

$$x_0' = -y_0(1-\eta). \tag{24}$$

These equations form a conservative system of equations with first integral

$$E_0 = \frac{x_0^2}{2(1-\eta)} + y_0 - \ln(1+y_0), \tag{25}$$

where E_0 is the constant of integration. For each $E_0 > 0$, there is a p-periodic orbit in the phase plane (x, y) surrounding the center $(x_0, y_0) = (0, 0)$. This first integral suggests to introduce the energy function defined by

$$E(x,y) \equiv \frac{x^2}{2(1-\eta)} + y - \ln(1+y). \tag{26}$$

Differentiating Eq. (26) with respect to time s and using Eqs. (17) and (18) give

$$E' = -\frac{\eta}{1-\eta}\theta x y' - \frac{\varepsilon x^2}{1-\eta}\left[1 + \frac{2P}{1-\eta}(1+y)\right] + O(\theta^2). \tag{27}$$

E' is $O(\varepsilon)$ small because θ is $O(\varepsilon)$. It motivates us to seek a perturbation solution for $E(s,\varepsilon)$ of the form $E = E_0(s) + \varepsilon E_1(s) + \cdots$. The leading equation is $E_0' = 0$ and implies that E_0 is constant. The $O(\varepsilon)$ problem for E_1 is

$$E_1' = -\frac{\eta}{1-\eta}\theta x_0 y_0' - \frac{\varepsilon x_0^2}{1-\eta}\left[1 + \frac{2P}{1-\eta}(1+y_0)\right], \tag{28}$$

where (x_0, y_0) is the p-periodic solution of Eqs. (23) and (24). In order that E_1 is a bounded function of s, the right hand side of Eq. (28) needs to satisfy the solvability condition

$$-\eta\theta\int_0^p x_0 y_0' ds - \varepsilon\int_0^p x_0^2\left[1 + \frac{2P}{1-\eta}(1+y_0)\right]ds = 0. \tag{29}$$

We use Eq. (23) to eliminate y_0' in Eq. (29). From Eq. (24), we determine y_0 as

$$y_0 = -\frac{x_0'}{1-\eta} \tag{30}$$

and realize that

$$\int_0^p x_0^2 y_0 ds = -\frac{1}{1-\eta}\int_0^p x_0^2 x_0' ds = 0. \tag{31}$$

Equation (29) then simplifies to

$$-\eta\theta\int_0^p x_0^2 ds - \varepsilon\left(1 + \frac{2P}{1-\eta}\right)\int_0^p x_0^2 ds = 0. \tag{32}$$

Factorizing the common integral, we find that

$$\theta = \varepsilon\theta_1, \tag{33}$$

where θ_1 is defined by Eq. (21), and all p-periodic solutions exhibiting different amplitudes are located at the same value of θ. In other words, the bifurcation is vertical to a first approximation and, to find how the amplitudes change with θ, a higher-order analysis is needed.

III. HIGHER-ORDER ANALYSIS

Toward this end, we first rewrite Eq. (18) as

$$x' = -y + \eta(y - \theta y') - \varepsilon x\left(1 + \frac{2P}{1-\eta}(1+y)\right) + \eta[y(s-\theta) - y + \theta y']. \tag{34}$$

We then use Eq. (17) to simplify y' in the third term of Eq. (34). We obtain

$$x' = -y + \eta(y - \theta\underline{x(1+y)}) - \varepsilon x\left(1 + \frac{2P}{1-\eta}(1+y)\right) + \eta[y(s-\theta) - y + \theta y'], \tag{35}$$

where the change has been underlined. We now wish to take advantage that the leading approximation of the Hopf bifurcation is $\theta = \varepsilon\theta_1$ where θ_1 is defined by Eq. (21). We introduce $\varepsilon^3\theta_3$ as the deviation of θ from $\varepsilon\theta_1$:

$$\theta = \varepsilon\theta_1 + \varepsilon^3\theta_3. \tag{36}$$

θ_3 multiplies ε^3 because the expression of the Hopf bifurcation point up to the third-order correction term is

$$\theta = \varepsilon\theta_1 + \varepsilon^3\frac{(1-\eta)\theta_1^3}{6} + O(\varepsilon^5), \tag{37}$$

where θ_1 is given by Eq. (21). We now note that the term $2P/(1-\eta)$ in Eq. (35) can be rewritten in terms of θ_1 as

$$\frac{2P}{1-\eta} = -\eta\theta_1 - 1. \tag{38}$$

Taking into account Eq. (38) and inserting Eq. (36) into Eq. (35) allow a substantial simplification. We find

$$x' = -y + \eta(y\underline{-\varepsilon^3\theta_3 x(1+y)}) + \underline{\varepsilon xy} + \eta[y(s-\theta) - y + \theta y'], \tag{39}$$

where the changes have been underlined. Reorganizing Eq. (39) in power series of ε and, together with Eq. (17), our dynamical problem takes the form

$$y' = x(1+y), \tag{40}$$

$$x' = -y(1-\eta-\varepsilon x) + R(x,y), \tag{41}$$

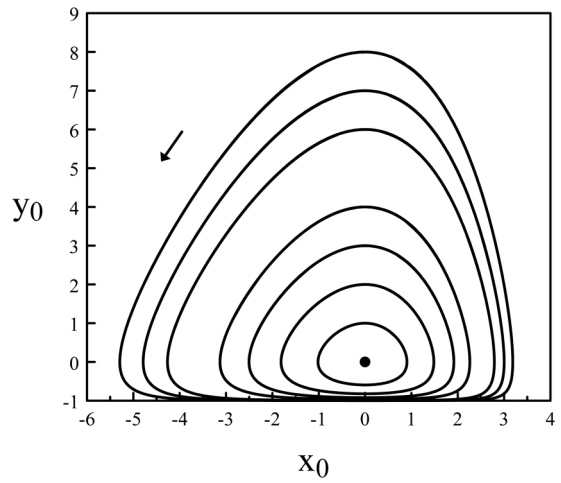

FIG. 4. Periodic orbits in the phase plane (x_0, y_0). They are the solutions of Eqs. (44) and (45) starting from the initial conditions $x_0(0) = 0$ and $y_0(0) = n$ $(n = 1, 2, \ldots)$. The arrow indicates the direction of the trajectories.

where

$$R(x, y) \equiv \eta[y(s-\theta) - y + \theta y'] - \eta\varepsilon^3\theta_3 x(1+y) \tag{42}$$

is an $O(\varepsilon^2)$-small quantity because the expression in brackets

$$[y(s-\theta) - y + \theta y'] = \frac{\theta^2}{2}y'' + O(\theta^3) \tag{43}$$

is $O(\varepsilon^2)$ since $\theta = O(\varepsilon)$. We proceed as in the previous section. Neglecting R, the reduced problem defined as

$$y_0' = x_0(1+y_0), \tag{44}$$

$$x_0' = -y_0(1-\eta-\varepsilon x_0) \tag{45}$$

admits a first integral. It suggests the new energy function

$$\overline{E}(x, y) \equiv y - \ln(1+y) - \frac{x}{\varepsilon} - \frac{1-\eta}{\varepsilon^2}\ln\left(\frac{1-\eta-\varepsilon x}{1-\eta}\right). \tag{46}$$

Differentiating $\overline{E}$ with respect to time s and simplifying using (40) and (41), we obtain

$$\overline{E}' = \frac{x}{1-\eta-\varepsilon x}R(x, y). \tag{47}$$

$\overline{E}'$ is $O(\varepsilon^2)$-small because $R(x, y)$ is $O(\varepsilon^2)$. Solvability requires that

$$\int_0^p \frac{x_0}{1-\eta-\varepsilon x_0}R(x_0, y_0)ds = 0, \tag{48}$$

where (x_0, y_0) now denotes the p-periodic solution of Eqs. (44) and (45) (see Fig. 4).

Equation (48) is the bifurcation equation which provides a relation between the amplitude and period of (x_0, y_0) and the bifurcation parameter θ_3. Our analysis indicates that the bifurcation analysis requires that the delayed variable is Taylor expanded up to third order. It suggests the derivation of a minimal set of ODEs with the same bifurcation properties as the original DDE problem.

IV. MINIMAL ORDINARY DIFFERENTIAL EQUATIONS

Equations (40)–(42) are the original DDEs reformulated as a weakly perturbed conservative system of equations. In the limit $\theta = O(\varepsilon) \to 0$. The Taylor expansion of the delayed variable $y(s-\theta)$ in Eq. (42) up to third order leads to the following expression for $R(x, y)$:

$$R = \eta\left[\frac{\varepsilon^2\theta_1^2}{2}y'' - \frac{\varepsilon^3\theta_1^3}{6}y'''\right] - \eta\varepsilon^3\theta_3 x(1+y) + \underline{O(\varepsilon^4)}. \tag{49}$$

It is mathematically convenient to evaluate y'' and y''' in terms of x and y We first compute y'' starting from Eq. (40) and evaluating the derivatives of x and y using Eqs. (40) and (41) [up to $O(\varepsilon^2)$ correction terms]. We sequentially find

$$\begin{aligned} y'' &= x'(1+y) + xy' \\ &= x'(1+y) + x^2(1+y) \\ &= -y(1-\eta-\varepsilon x)(1+y) + x^2(1+y) + \underline{O(\varepsilon^2)}. \end{aligned} \tag{50}$$

To compute y''', we start with y'' given by Eq. (50) up to $O(\varepsilon)$ corrections. It is given by

$$y'' = -(1+y)y(1-\eta) + x^2(1+y) + \underline{O(\varepsilon)}. \tag{51}$$

We then again use Eqs. (40) and (41) to simplify the time derivatives of x and y [up to $O(\varepsilon)$ corrections terms]. We obtain

$$\begin{aligned} y''' &= -(1-\eta)(1+2y)y' + 2xx'(1+y) + x^2y' + \underline{O(\varepsilon)} \\ &= -(1-\eta)(1+2y)x(1+y) - 2x(1+y)y(1-\eta) \\ &\quad + x^3(1+y) + \underline{O(\varepsilon)} \\ &= -(1-\eta)(1+4y)x(1+y) + x^3(1+y) + \underline{O(\varepsilon)}. \end{aligned} \tag{52}$$

The minimal ODE problem is given by Eqs. (40) and (41), where R is now given by

$$\begin{aligned} R = \eta\begin{bmatrix} \frac{\varepsilon^2\theta_1^2}{2}\begin{pmatrix} -y(1-\eta-\varepsilon x)(1+y) \\ +x^2(1+y) \end{pmatrix} \\ -\frac{\varepsilon^3\theta_1^3}{6}\begin{pmatrix} -(1-\eta)(1+4y)x(1+y) \\ +x^3(1+y) \end{pmatrix} \end{bmatrix} \\ - \eta\varepsilon^3\theta_3 x(1+y) + \underline{O(\varepsilon^4)}, \end{aligned} \tag{53}$$

where the neglected terms are all $O(\varepsilon^4)$.

It is worthwhile to discuss the significance of each term in Eq. (53). From Eqs. (40) and (41), we formulate the linearized equations with $R(x, y)$ given by Eq. (53). They are

$$y' = x, \tag{54}$$

$$\begin{aligned} x' = &-y(1-\eta) + \eta\left[-\frac{\varepsilon^2\theta_1^2}{2}y(1-\eta) + \frac{\varepsilon^3\theta_1^3}{6}(1-\eta)x\right] \\ &- \eta\varepsilon^3\theta_3 x. \end{aligned} \tag{55}$$

The first and second terms in Eq. (55) provide the leading term of the Hopf bifurcation point and the $O(\varepsilon^2)$ correction of its frequency, respectively. The third term gives the $O(\varepsilon^3)$ correction of Hopf bifurcation point [see Eq. (37)].

The numerical bifurcation diagram of Eqs. (40) and (41) with Eq. (53) is shown in Fig. 5 in red. It is compared with the diagram obtained from the original DDE problem (40)–(42) (in blue). The agreement is quantitative because

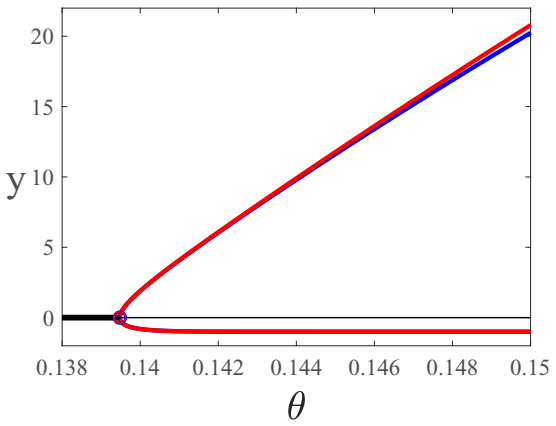

FIG. 5. Numerical bifurcation diagram for $P = 0.1$, $\eta = -0.5$, $T = 2000$. Blue: extrema of periodic orbits of Eqs. (40)–(42) using a continuation technique [26]. Red: extrema of periodic orbits of Eqs. (40) and (41) with the reduced $R(x, y)$ given by Eq. (53). Bold (thin) black line is stable (unstable) steady state. The red and blue circles indicate the Hopf bifurcation points.

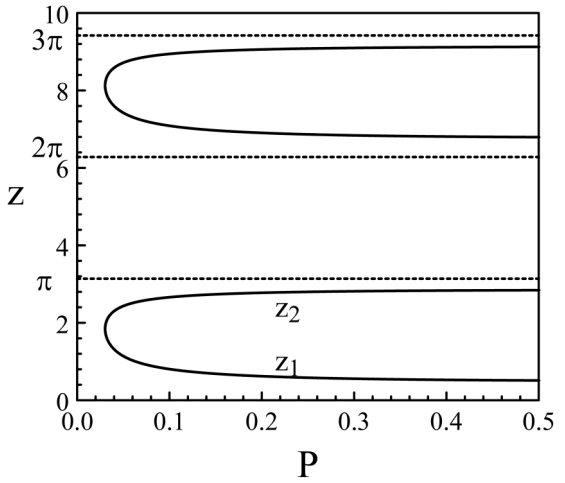

FIG. 6. Hopf bifurcation curves in terms of $z = \sigma\tau$ and P. They are obtained from the Hopf bifurcation conditions (9) and (10).

$T = 2000$ implies, using Eq. (19), a small $\varepsilon \simeq 0.06$. We may also compare the exact numerical value of the bifurcation point and its approximation (37). We find $\theta_{\text{num}} = 13.954$ and $\theta_{\text{app}} = 13.947$ indicating a minor difference of 0.007.

V. DISCUSSION

Many lasers (semiconductor lasers and solid-state lasers) operate in the so-called class B regime, with the upper-state lifetime being much longer than the cavity damping time. In that regime, pump power changes lead to slowly damped but pronounced relaxation oscillations (ROs). They are found numerically by simulating similar nonlinear rate equations, and they are analyzed mathematically as weakly damped conservative oscillations [25]. It was recently reported that ROs may be sustained by a time-delayed feedback exhibiting a short delay and a strong feedback gain. The Hopf bifurcation transition has been observed both experimentally and numerically by using a dual-polarization fiber laser submitted to a time-delayed frequency-shifted optical feedback [27]. The two-mode laser exhibits time constants typical of a Class B laser, and the simulated four rate equations are actually in the form of two coupled weakly damped conservative system of equations similar to Eqs. (17) and (18).

Recently developed on-chip technologies may potentially allow integrated optoelectronic feedback with nearly arbitrary delays. It motivated us to consider a semiconductor laser subject to a time-delayed optoelectronic feedback, which is described by only two equations. The limit of short delays is realized for negative delayed feedback and by decreasing the relaxation oscillation frequency. This is possible by operating the laser close to threshold [18].

In this paper, we showed that the Hopf bifurcation instability is possible when the short delay is comparable to the small damping rate of the ROs. In other words, the delayed feedback with a short delay but moderate amplitudes has a destabilizing effect that compensates the stabilizing effect of the weak damping of the ROs. This is clearly transparent in the bifurcation equation (29) where the terms multiplying ε and θ represent the effects of the RO damping and the delayed feedback, respectively. The Hopf bifurcation nature is nonconventional because the bifurcating branch is nearly vertical, meaning that the oscillations quickly change from harmonic to pulsating as the control parameter deviates from its bifurcation point. To resolve this difficulty, we had to expand the delayed variable for small delays up to third order and derive two successive bifurcation equations. Our analysis opens the way to new applications using moderate to strong optoelectronic feedbacks but short delays.

ACKNOWLEDGMENTS

The work of A.V.K. and E.A.V. was supported by the Ministry of Science and Higher Education of the Russian Federation, research Project no. 2019-1442.

APPENDIX: HOPF BIFURCATION CONDITIONS

In this Appendix, we further analyze the Hopf bifurcation conditions (9) and (10). Figure 6 shows z as a function of P. We denote by z_1 and z_2 the two first branches of solutions. The other branches verify the relation

$$z_n = z_1 + 2n\pi \text{ and } z_m = z_2 + 2m\pi \ (n, m = 1, 2, \ldots). \quad \text{(A1)}$$

To demonstrate (A1), we rewrite Eq. (10) as

$$P = -\frac{1}{2}\frac{1-\eta}{1+\eta\frac{\tau}{z}\sin(z)}. \quad \text{(A2)}$$

From Eq. (7), we determine τ/z given by

$$\frac{\tau}{z} = -\frac{(1-\eta)T}{2P[\eta\cos(z)-1]}. \quad \text{(A3)}$$

Inserting (A3) into Eq. (A2) leads to

$$P = -\frac{1}{2}\frac{1-\eta}{1+\eta\sin(z)\sqrt{-\frac{(1-\eta)T}{2P(\eta\cos(z)-1)}}}. \quad \text{(A4)}$$

Simplifying, we obtain

$$P^{1/2} = -\frac{\sqrt{(1-\eta\cos(z))(1-\eta)}}{1+\eta\sin(z)\sqrt{2(1-\eta)T}}. \tag{A5}$$

P now depends on z only through the trigonometric functions. Therefore, every z satisfying (A1) admits the same value of P.

We next demonstrate that Eq. (A1) also implies that there are only two frequencies $\sigma_1 = \sigma_1(z_1)$ and $\sigma_2 = \sigma_2(z_2)$. We rewrite Eq. (10) by inserting $z = \sigma\tau$ and factorizing τ^2

$$[1-\eta\cos(z)] + \eta\sin(z)T\sigma + \sigma^2 T = 0. \tag{A6}$$

This equation does not depend on P and τ only appears through z in the trigonometric functions. This then implies that all z satisfying Eq. (A1) lead to the same value of σ.

[1] M. C. Soriano, J. García-Ojalvo, C. R. Mirasso, and I. Fischer, Complex photonics: Dynamics and applications of delay-coupled semiconductors lasers, Rev. Mod. Phys. **85**, 421 (2013).

[2] M. Sciamanna and K. A. Shore, Physics and applications of laser diode chaos, Nat. Photonics **9**, 151 (2015).

[3] D. M. Kane and K. A. Shore (Eds.), *Unlocking Dynamical Diversity* (John Wiley & Sons, Chichester, 2005).

[4] J. Ohtsubo, *Semiconductor Lasers*, 4th ed. (Springer International Publishing, Cham, 2017).

[5] K. Lüdge and B. Lingnau, Laser dynamics and delayed feedback, in *Encyclopedia of Complexity and Systems Science*, edited by R. Meyers (Springer, Berlin, Heidelberg, 2020), pp. 1–18.

[6] K. Ikeda, Multiple-valued stationary state and its instability of the transmitted light by a ring cavity system, Opt. Commun. **30**, 257 (1979).

[7] K. Ikeda, H. Daido, and O. Akimoto, Optical Turbulence: Chaotic Behavior of Transmitted Light From a Ring Cavity, Phys. Rev. Lett. **45**, 709 (1980).

[8] S.-N. Chow, J. K. Hale, and W. Huang, From sine waves to square waves in delay equations, Proc. - R. Soc. Edinburgh, Sect. A: Math. **120**, 223 (1992).

[9] J. Hale and W. Huang, Period doubling in singularly perturbed delay equations, J. Differ. Equ. **114**, 1 (1994).

[10] J. Gao, J. Yuan, and L. Narducci, Instabilities and chaotic behavior in a hybrid bistable system with a short delay, Opt. Commun. **44**, 201 (1983).

[11] F. T. Arecchi, G. Giacomelli, A. Lapucci, and R. Meucci, Dynamics of a CO_2 laser with delayed feedback: The short-delay regime, Phys. Rev. A **43**, 4997 (1991).

[12] T. Heil, I. Fischer, W. Elsäßer, and A. Gavrielides, Dynamics of Semiconductor Lasers Subject to Delayed Optical Feedback: The Short Cavity Regime, Phys. Rev. Lett. **87**, 243901 (2001).

[13] T. Heil, I. Fischer, W. Elsäßer, B. Krauskopf, K. Green, and A. Gavrielides, Delay dynamics of semiconductor lasers with short external cavities: Bifurcation scenarios and mechanisms, Phys. Rev. E **67**, 066214 (2003).

[14] A. Tabaka, K. Panajotov, I. Veretennicoff, and M. Sciamanna, Bifurcation study of regular pulse packages in laser diodes subject to optical feedback, Phys. Rev. E **70**, 036211 (2004).

[15] C. Otto, B. Globisch, K. Lüdge, E. Schöll, and T. Erneux, Complex dynamics of semiconductor quantum dot lasers subject to delayed optical feedback, Int. J. Bifurcation Chaos Appl. Sci. Eng. **22**, 1250246 (2012).

[16] K. Takano, C. Sugano, M. Inubushi, K. Yoshimura, S. Sunada, K. Kanno, and A. Uchida, Compact reservoir computing with a photonic integrated circuit, Opt. Express **26**, 29424 (2018).

[17] S. Bauer, O. Brox, J. Kreissl, B. Sartorius, M. Radziunas, J. Sieber, H.-J. Wünsche, and F. Henneberger, Nonlinear dynamics of semiconductor lasers with active optical feedback, Phys. Rev. E **69**, 016206 (2004).

[18] J. P. Toomey, D. M. Kane, C. McMahon, A. Argyris, and D. Syvridis, Integrated semiconductor laser with optical feedback: Transition from short to long cavity regime, Opt. Express **23**, 18754 (2015).

[19] G.-Q. Xia, S.-C. Chan, and J.-M. Liu, Multistability in a semiconductor laser with optoelectronic feedback, Opt. Express **15**, 572 (2007).

[20] Y. K. Chembo, D. Brunner, M. Jacquot, and L. Larger, Optoelectronic oscillators with time-delayed feedback, Rev. Mod. Phys. **91**, 035006 (2019).

[21] F. yi Lin and J.-M. Liu, Nonlinear dynamics of a semiconductor laser with delayed negative optoelectronic feedback, IEEE J. Quantum Electron. **39**, 562 (2003).

[22] D. Pieroux, T. Erneux, and K. Otsuka, Minimal model of a class-*B* laser with delayed feedback: Cascading branching of periodic solutions and period-doubling bifurcation, Phys. Rev. A **50**, 1822 (1994).

[23] D. Pieroux and T. Erneux, Strongly pulsating lasers with delay, Phys. Rev. A **53**, 2765 (1996).

[24] A. V. Kovalev, M. S. Islam, A. Locquet, D. S. Citrin, E. A. Viktorov, and T. Erneux, Resonances between fundamental frequencies for lasers with large delayed feedbacks, Phys. Rev. E **99**, 062219 (2019).

[25] T. Erneux and P. Glorieux, *Laser Dynamics* (Cambridge University Press, Cambridge, 2010).

[26] K. Engelborghs, T. Luzyanina, and D. Roose, Numerical bifurcation analysis of delay differential equations using DDE-BIFTOOL, ACM Trans. Math. Softw. **28**, 1 (2002).

[27] M. Guionie, M. Romanelli, A. Thorette, A. Carré, E. Pinsard, L. Lablonde, B. Cadier, M. Alouini, M. Vallet, and M. Brunel, Delay-induced instability in phase-locked dual-polarization distributed-feedback fiber lasers, Phys. Rev. A **101**, 043843 (2020).